NAME: Mioto Takahashi
DATE: May 1, 2024 (Modified on April 30, 2025)
Final Project
Data Science II

Abstract

The detection and inference of the cause of convergence in anatomical features between phylogenetically distant taxa or clades is a topic of research in the field of ontogeny and phylogeny. Preliminary research have proposed hypotheses in the role of head-body proportions and head ornaments in ceratopsians and extant quadrupedal animals; however, whether there are signs of convergent evolution between the two clades is an open problem. Similarities in skull length, femur length, femur circumference, and humerus length of taxa within the clades are analyzed using principal component analysis, Bayesian inference, Kolmogorov-Smirnov test, and Mann-Whitney-Wilcoxon U-test.

1 Introduction

Convergent evolution of similar anatomical characteristics between extinct archosaurs and extant mammals have been a topic of research. Preliminary works have focused on inter-species allometry, such as the similarities in head-to-body ratio between the two groups, and intra-species characteristics, such as the similarities in the shape of head ornaments within ceratopsians. However, whether ceratopsians have any non-superficially similar characteristics to extant mammals is an open problem. Convergent evolution can be simulated using evolutionary algorithms, where the fitness function would be a representation of biological species' survival, and the solutions would be the existing species observed in field studies. Understanding the similarity of the two leading hypotheses for the use of head ornaments, defensive mechanisms and reproduction pressure, between two phylogenetically distant groups can give insight into the fitness landscape of biological ecosystems. Similarity in characteristics between ceratopsians and extant mammals indicate that the two groups have similar biological fitness functions. In this project, whether the head-body anatomy of ceratopsians and extant mammals are a result of convergent evolution is analyzed by comparing the distributions of anatomical measurements, regarding heads and bodies, between ceratopsians and extant mammals. The difference between the two distributions indicate the similarities between the two groups. If the difference is small, the hypotheses regarding the functionalities of the head ornaments in ceratopsians will be implied to be similar to those of extant mammals. The difference of distributions are calculated with the use of both Kolmogorov-Smirnov test and Mann-Whitney-Wilcoxon U-test to avoid p-hacking and arriving to false conclusions.

2 Preliminary Works

2.1 Inference of Convergent Evolution via Data Analysis of Anatomical Measurements

Hypotheses regarding the functionalities of anatomical characteristics in extinct animals have been tested using related anatomical measurements.

A hypothesis in which the syncervical vertebrae, or fused cervical vertebrae found in ceratopsians, were used to support the impact force on their large heads during head-to-head combat was tested [26]. Measurements of skull mass, body mass, basal skull length, length of cervical vertebral series, etc. of 45 quadruped taxa of 26 mammals and 19 reptiles were used to determine their relative head sizes, and compared with the measurements for 5 ceratopsian species and 15 other dinosaur species. Linear regressions that capture the correlations between each measurement and comparing the residual distribution between each group was conducted. It was concluded that the skull size and evolutionary development of cervical weaponry, or the horns and frills, do not correlate with the increase in the size of the syncervical vertebrae, rejecting the aforementioned hypothesis. Our project shifts the focus from analysis of intra-species syncervical vertebrae to interspecies body mass and limb proportions.

The correlation between occipital condyle width (OCW), or the width of the occipital bone found at the base of the skull, and the body mass of extant terrestrial mammals were tested using curvelinear regression, and was found that the OCW was able to accurate estimate the body mass [6]. In our project, the range of extant taxa is expanded to include reptiles.

For developing methods of better body mass estimation, the proportions between limb length and body mass were compared between extant mammals and reptiles, and the similarities in anatomical measurements between phylogenetically distant clades were measured [4]. Measurements of humerus, femur, and other anatomical features were put through logarithms and linearly regressed to body mass. While the limb proportions and limb length to body mass ratio are different between the two groups, the proportions of circumference of the proximal limb bones, or the humerus and femur, and body mass ratio are found to have similarities. Our project adds an extant clade, ceratopsians, to see any sign of convergent evolution between such and extant quadrupedal taxa. Alternative methods of body measurement predictions have been proposed for different clades [25] [17].

Anatomical data has been used to make inferences about phenotypic evolution. A single specimen of an early mosasaur, an aquatic archosaur, platecarpus was investigated and compared with modern terrestrial lizards and extant sharks, where anatomical similarities between the two species were found [11]. It was discussed that locomotion may have lead to the convergence in anatomy, mainly the heart between platecarpus and terrestrial lizards and the tail fin between platecarpus and sharks. Alternatively, DNA from128 feather samples from a pigeon genus Columba livia and a dove genus Streptopelia risoria were collected and extracted for analysis of the genetic cause of their head crests, where it was hypothesized that there may have been selection pressure to encourage mutation that cause development of anatomical features with similar functionalities [27].

The use of principal component analysis can help visualize the distribution of high dimensional data of shapes of anatomies. Anatomical wireframes of anolis skulls were measured and mapped to 3 principal components to analyze the clade's sexual dimorphism, where it was found that clades carolinensis and hendersoni have similar patterns of sexual dimorphism, specifically male-specific changes in facial features, despite differences in developmental processes between the clades [23]. The geometry of manibles, or jawbones, and crania, or skull, of extant and extinct adult durophages, or animals that feed on hard-shelled prey, were measured using interlandmark distances within their image data and were analyzed using principal component analysis, where it was found that the durophages had similar skeletal structures regardless of their phylogenetic distances [7]. Body mass, centroid, bite force, and other measurements alongside landmark data on 3-D scans of the crania of non-herbivorous marsupial and carnivorous placental genus were put through generalized Procrustes Superimposition and Principal Component Analysis, which allowed visualization of "mean" shapes along the axes of the eigenspaces [28].

Environmental data can be appended to anatomical data to make inferences on the functionalities of the said anatomy. Geometric data of adult Thomomys specimen, a species of fossorial mammals as characterized by their behavior of digging into soil, and soil data of environments inhabited by the specimen were analyzed using principal component analysis. Convergent evolution in incisor procumbency, or the frontal teeth present in rodents, was found in varying sizes of Thomomys residing in environments with hard soils, regardless of the tendencies for the skull shapes to change with little allometric changes [13]. Skull shapes of crocodilian and Odontoceti, or toothed whale, specimen were compared to analyze the cause of the similarities and convergent evolution in the shapes. Landmarks assigned in CT scans of mandibles and crania of the specimen from the two clades were applied to procrustes superimposition, a geometric statistical analysis method, and linearly regressed to diet, habitat, and prey size, where it was found that diet may be driving the convergent evolution in skull shape variation between the clades [14].

Anatomical variation of clades has been the subject of comparison for analysis of convergent evolution. The phenotypic variation in bodies of two phylogenetically distant species of true flies, Prochyliza xanthostoma and Telostylinus angusticollis were compared to evaluate whether a common feature in sexual dimorphism, specifically male body elongation, is similar between the two species and is a sign of convergent evolution [2].

2.2 Anatomy Functionalities and Evolution

Ceratopsians are known for their characteristic horns and frills, and their functionalities and evolutionary significance has been a topic of research. Oxygen isotopie composition of bones and frills of triceratops were analyzed, where it was hypothesized that they were used for thermoregulation [21]. Ceratopsians may have used their jaws akin to shears for processing resilient fiber-like plants, and the difference in kinematics between centrosaurinae, an earlier clade associated with short frills, and chasmosaurinae, an advanced clade associated with long rills, may have resulted in the differences in size of their frills for different levels of muscular support of the mandible [18].

Analyses of extinct and extant taxa have been used to make hypotheses about the role of cranial geometry. The differences in asymmetry of horns in gazelles were indicative of functionality in sexual competition [16]. The mandible and the upper tooth row of Rhinocerotinae had high covariance with the hypsodonty and low covariance with phylogeny, and the skull shape had an inverse relationship with the hypsodonty, hinting that the anatomical parts for mastication, or chewing is mostly dictated by the functionality rather than evolutionary morphologic development [19]. The variation in cranial measurements of Calomys musculinus were found to be different between sexes and locations, where the male specimen between different localities showed significantly more variation than the other groups, indicating the role the social selection pressure in development [20].

While focus on a specific feature in anatomy may reveal important information about its functionality, it is important to take morphological integration, or traits that emerge due to coordination with other features in the body [24].

The evolution of allometry, or heterochrony, has been studied by utilizing measurement proportions [9]. Measurements of forelimbs, hind limbs, and body sizes in archosaurs have been used to indicate that the scaling of limbs were separated from the body in early diversification of birds resulting in an evolution of powered flight [5]. Alternatively, the differences in habitat have been hypothesized to affect allometry [10]. In the case of Anolis lizards, development of limb proportions between species were due to formation of cartilage earlier in evolution [22]. Positive allometry, or disproportions in allometry, can emerge when the anatomical feature that is showing in proportions can cause increase the marginal fitness, the main cause being sexual selection [3].

Limb proportions have been linked to locomotion in preliminary studies. Osteology, or the study of skeletal structure, revealed that quarupedalism in archosaurs were evolutionarily ancient, meaning that bipedalism should have been developed at least once in both the crocodilian and bird specimens, while myology, or the study of muscular structure, although difficult to analyze due to the easiness of obtaining inaccurate assumptions about muscular sizes, connections, etc., revealed that archosaurus may have evolved from hip-based locomotion to knee-based locomotion.[8]. Allometry can be affected by both selection pressure and ontogeny [1]. Additionally, such studies have been applied to aquatic locomotion [29].

Situations in which phenotypic convergent evolution can emerge has been discussed preliminarily. Convergent evolution can occur from different genes segments, even within the same clades, and distantly related species [12]. The same study additionally highlights that the same genes do not require to mutate in the same way to produce similar phenotypes.

3 Data

The Ceratopsian Dataset containing basal skull length, femur length, and humerus length for 55 ceratopsian taxa are provided by Vanburen et al. [26]. The characteristic large frills in ceratopsians are taken into account of the skull lengths. Dropping taxa with NaN values result in 20 taxa 1, indicating the lack of accuracy for model construction for imputation with a limited number of dataset.

Additionally, Dino Dataset containing similar measurements of extinct dinosaurs, extant reptiles, and extant mammals are provided by the same paper. Out of the 118 taxa are listed, 53 have no NaN values and are usable. All 53 taxa were found to be either extant reptiles or extant mammals. However, this dataset does not include the humerus length, but instead additionally has femur circumference and humerus

	Taxon	Femur Length	Humerus Length	Skull Length
0	Hypsilophodon	173.00	147.0	118.882
1	Stegoceras	225.00	86.0	192.000
2	Yinlong	155.00	91.0	163.276
3	Psittacosaurus_mongoliensis	162.00	119.0	186.571
4	Psittacosaurus_sinensis	96.00	82.0	113.000
5	Psittacosaurus_neimongoliensis	130.00	105.0	132.000
6	Psittacosaurus_major	172.00	149.0	203.000
7	Protoceratops	330.00	215.0	702.000
8	Centrosaurus	795.00	563.0	1372.000
9	Triceratops	1160.00	750.0	1940.000
10	Cerasinops	352.00	260.3	334.934
11	Montanoceratops	346.00	263.0	467.126
12	Udanoceratops	525.65	361.5	654.085
13	Leptoceratops	285.00	248.0	455.000
14	Auroraceratops	153.00	119.0	188.333
15	Chasmosaurus_belli	920.00	671.0	1930.000
16	Pentaceratops	1020.00	859.0	2723.080
17	Utahceratops	940.18	596.5	2464.110
18	Chasmosaurus_russelli	716.00	563.0	1480.000
19	Avaceratops	395.00	290.0	813.740
20	Styracosaurus	792.00	585.5	1950.000

Figure 1: Ceratopsian Dataset without NaN

circumference.

Mammal Dataset, referring to the dataset provided by [6], contains the skull length, head-body length, or total body length, and body mass for 404 extant mammalian taxon. None of the samples include NaN values; however measurements regarding the femur and humerus are not taken into consideration.

Quadruped Dataset, provided by [4], contains the phylogenetic family, higher-order clade, femur length, femur circumference, humerus length, humerus circumference, and body mass for 241 extant reptilian and mammalian quadrupedal taxa 2. With the family and higher clade columns, possibility of making subgroups for smaller distributions may be possible.

All lengths in the 4 datasets are in millimeters and all masses are in grams.

4 Method

Given that the Ceratopsian and Quadruped Datasets, both have femur length and humerus length, they are mainly used to compare measurements between ceratopsians and extant mammals. Additional features, femur circumference for the Ceratopsian Dataset and skull length for the Quadruped Dataset, are estimated and imputed using curve regression models for comparison.

	Higher Clade	Family	Taxon	Femur Length	Femur Circumference	Humerus Length	Humerus Circumference	Body Mass
0	Afrotheria	Elephantidae	Elephas_maximus	980.00	315.00	830.00	310.00	3534000.0
1	Afrotheria	Elephantidae	Loxodonta_africana	1147.50	399.00	1035.00	416.30	6435000.0
2	Afrotheria	Macroscelididae	Petrodromus_tetradactylus	47.30	12.50	33.70	9.50	275.0
3	Afrotheria	Procaviidae	Heterohyrax_brucei	79.50	24.25	78.20	21.75	3650.0
4	Carnivora	Canidae	Alopex_lagopus	114.68	24.85	112.15	23.00	3710.0
...	...	...	...	...	...	...	...	...
236	Amphibia	Bufonidae	Rhinella_schneideri	52.20	12.15	45.05	11.90	538.0
237	Amphibia	Leptodactylidae	Lepidobatrachus_laevis	35.70	8.50	32.40	8.50	166.8
238	Amphibia	Hylidae	Osteopilus_septentrionalis	53.80	7.70	32.10	8.50	117.0
239	Amphibia	Pipidae	Xenopus_laevis	30.00	7.90	14.80	5.40	109.5
240	Amphibia	Microhylidae	Dyscophus_guineti	28.00	6.20	19.50	6.60	76.0

Figure 2: Quadruped Dataset without NaN

While the Quadruped Dataset and the Mammal Dataset both contain the body mass of each taxon, only the latter contains the skull length. Additionally, while the Quadruped Dataset and the Dino Dataset both contain the femur length, femur circumference, and humerus circumference, only the latter contains the skull length. Curve regression models for predicting the skull length in the Quadruped Dataset, from body mass and from femur length, femur circumference, and humerus circumference, can be constructed using the Mammal Dataset and the Dino Dataset, respectively. The two regressed models are weighed with the negative mean squared losses of each model put through a softmax function.

Similarly, the Ceratopsian Dataset and the Dino Dataset both contain the femur length and the skull length, while only the latter contains the femur circumference. The 3 variables in the Dino Dataset is put through a curve regression for estimating the femur circumference in the Ceratopsian Dataset.

For each curve regression model construction, the model with the least estimated mean squared error out of log-linear, log-quadratic, and log-cubic functions is selected. The error estimate for each model is calculated via 10-fold cross validation. While log-exponential regression is additionally used for model selection in preliminary research [6], this is ignored due to the low predictive performance (figure 3).

The imputed Quadruped and Ceratopsian Datasets both consist of the femur length, femur circumference, humerus length, and skull length. The 4 features are put through principal component analysis (PCA), where the principal components are selected using Minka's MLE [15].

The resulting variables are used to fit to a Bayesian model described as the following.

Set X as the values of all principal components $(x_{PC1}, x_{PC2}, x_{PC3})$. The support of each variable is

$$x_{PC1} \in [0, \infty) \cap \mathbb{R} \tag{1}$$
$$x_{PC2} \in (-\infty, \infty) \cap \mathbb{R} \tag{2}$$
$$x_{PC3} \in (-\infty, \infty) \cap \mathbb{R}, \tag{3}$$

where each principal component is assumed to be independent.

Aligning with the aforementioned support, the likelihood of X is

$$x_{PC1} \sim Normal^{+}(\alpha_{PC1}, \sigma_{PC1}) \tag{4}$$
$$x_{PC2} \sim Normal(\alpha_{PC2} x_{PC1} + \beta_{PC_2}, \sigma_{PC2}) \tag{5}$$
$$x_{PC3} \sim Normal(\alpha_{PC3} x_{PC2} + \beta_{PC_3}, \sigma_{PC3}), \tag{6}$$

where α_{PC2} and α_{PC3} are the slopes and β_{PC2} and β_{PC3} are the intercepts of the corresponding linear regressors.

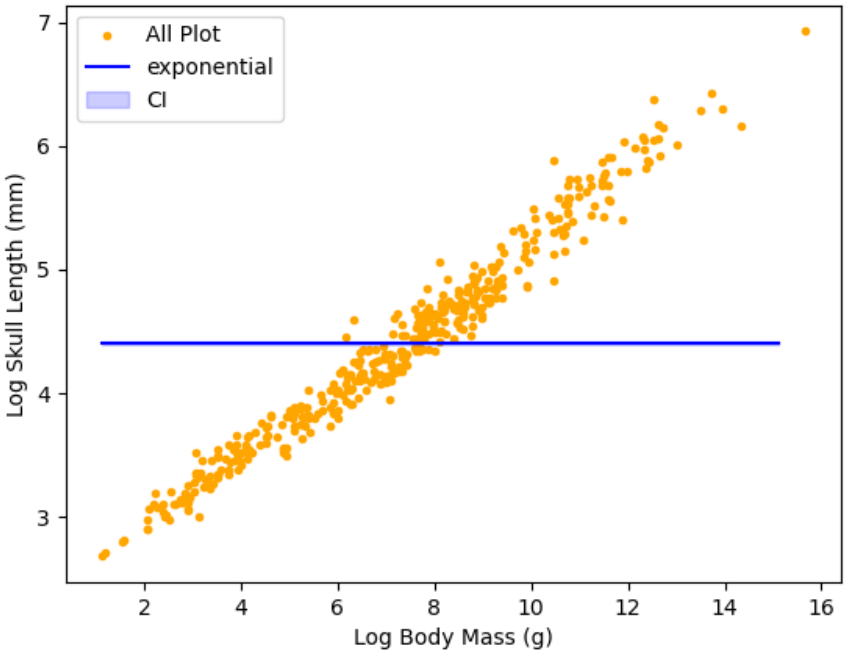

Figure 3: An example result of performing exponential regression on skull length and body mass in the Mammal Dataset

The priors for $\alpha = (\alpha_{PC1}, \alpha_{PC2}, \alpha_{PC3})$ and $\beta = (\beta_{PC2}, \beta_{PC3})$ are set as

$$\alpha_{PC1} \sim Normal^{+}(a_{1PC1}, a_{2PC1}) \tag{7}$$
$$\alpha_{PC2} \sim Normal(a_{1PC2}, a_{2PC2}) \tag{8}$$
$$\alpha_{PC3} \sim Normal(a_{1PC3}, a_{2PC3}) \tag{9}$$
$$\beta \sim Normal(b_1, b_2) \tag{10}$$
$$a_{1PC1} \sim Normal^{+}(0.0, 1.0) \tag{11}$$
$$a_{1PC2,PC3}, b_1 \sim Normal(0.0, 1.0) \tag{12}$$
$$a_2, b_2 \sim Exponential(1.0) \tag{13}$$

The prior for $\sigma = (\sigma_{PC1}, \sigma_{PC2}, \sigma_{PC3})$ is set as

$$\sigma \sim Gamma(s_1, s_2) \tag{14}$$
$$s_1 \sim Exponential(1/\mu') \tag{15}$$
$$s_2 \sim Exponential(1.0). \tag{16}$$

μ' is set as $[100, 1, 1]$ for each principal component.

The posteriors for the Bayesian linear regression model are sampled using Hamiltonian Monte Carlo Markov Chain (MCMC) . The sampled points are compared between the models fit to Quadruped and Ceratopsian Dataset using Kolmogorov-Smirnov (KS) test, and Mann-Whitney-Wilcoxon U-test, whose null hypothesis is that the 2 sample distributions have the same parent distribution. The rejection of the

null hypothesis indicates that the difference between the body proportions of the 2 clades are statistically significant and there is no evidence of convergent evolution.

5 Results

5.1 Data Imputation

Mean squared loss estimates for linear, quadratic, and cubic functions calculated using 10-fold cross validation were calculated.

The 10-fold cross validation and test losses for the skull length estimations via linear, quadratic, and cubic regressions using the Mammal Dataset are as table 1 and figure 4. The quadratic model has the least error for both the validation and test data; therefore, this model is selected for imputation. The quadratic model trained on all available data in the Mammal Dataset had a loss of 0.1982.

	Validation		Test	
	MSE	CI	MSE	CI
Linear	0.0214	0.0003	0.0217	0.0033
Quadratic	0.01949	0.0004	0.0200	0.0041
Cubic	0.01960	0.0004	0.0201	0.0041

Table 1: Average mean squared error (MSE) losses and their confidence intervals (CI) of linear, quadratic, and cubic regression models for skull length estimations from body mass are trained using the Mammal Dataset.

Regression models for the skull length estimations using the Dino Dataset are as table 2 and figures 5, 6, and 7. While the cubic function has the lowest loss for the validation data, the linear function has the lowest loss for the test data, indicating that the quadratic and cubic models tend to overfit in this particular task. The linear model trained on all available data in the Dino Dataset was 0.0635.

The negative estimate losses of the skull length estimators trained on Mammal and Dino Dataset put into a softmax function resulted in 0.5110 and 0.4890, respectively. These values were used as weights for estimating the skull length in the Quadruped Dataset.

	Validation		Test	
	MSE	CI	MSE	CI
Linear	0.0625	0.0041	0.0847	0.0475
Quadratic	0.0580	0.0039	0.0959	0.0499
Cubic	0.0537	0.0042	0.1455	0.0829

Table 2: Average mean squared error (MSE) losses and their confidence intervals (CI) of linear, quadratic, and cubic regression models for skull length estimations from femur circumference, femur length, and humerus circumference are trained using the Dino Dataset.

Regression models for the femur circumference estimations using the Dino Dataset are as table 3 and figures 8, 9, and 10. While the cubic function has the lowest loss for the validation data, the linear function has the lowest loss for the test data, indicating that the quadratic and cubic models tend to overfit in this particular task. The linear model trained on all available data in the Dino Dataset was 0.0400.

5.2 Distribution Fitting and Comparison

The 4 features were reduced to 3 using principal component analysis (figure 11).

The prior predictive check is as figure 12.

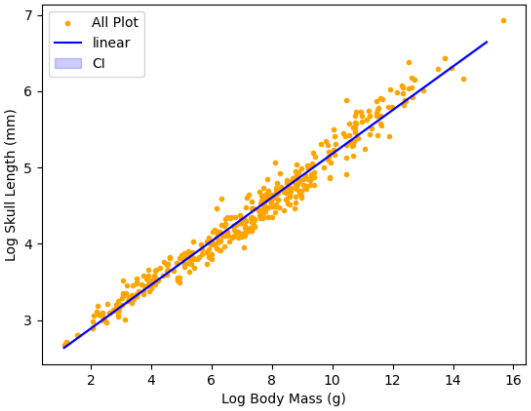

(a) Linear function

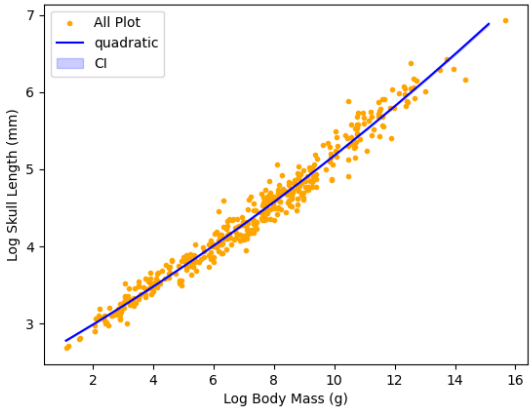

(b) Quadratic function

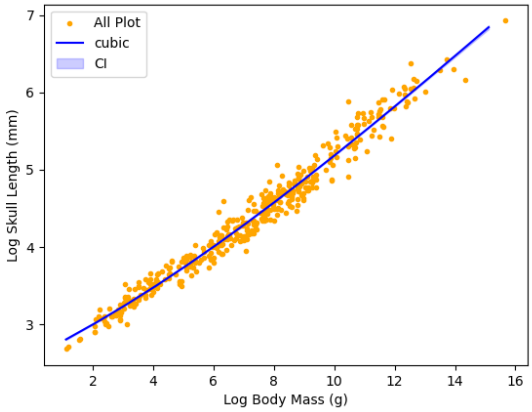

(c) Cubic function

Figure 4: Regression plots for skull length estimations from body mass trained using the Mammal Dataset.

The $\hat{r}$ values for the points sampled from the posterior using MCMC for all parameters were within $(0.09, 1.01)$, indicating convergence in the values and that the Bayesian linear regression models were able to fit to the 2 datasets. The plots for the posterior predictive check is as 13.

The inferred distributions corresponding to the two datasets were sampled and plotted onto the eigenspace alongside the preexisting taxa (figure 11). The plot shows the points sampled from the distributions overlapping with the taxa from the corresponding datasets.

The p-values per each principal component for the KS test and the Mann-Whitney-Wilcoxon U-test are as **??**. All of the null hypotheses were rejected, indicating that the parent distributions for the models fit to Quadruped and Ceratopsian datasets are not equal.

6 Discussion

Looking at the loss of the skull length regressors, both body mass and femur length, femur circumference, and humerus circumference were nearly equally accurate at producing estimations. With the former regressor being quadratic and the latter being linear, while the allometry may be static regarding length, bigger body

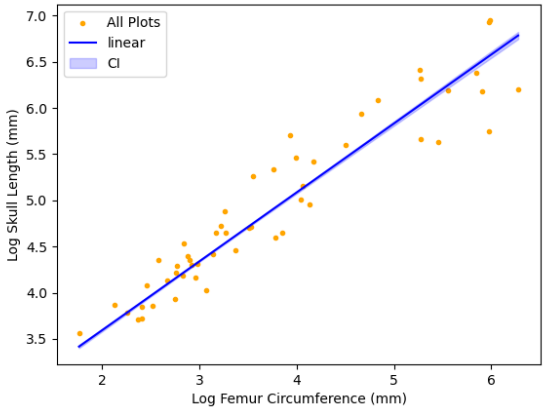

(a) Femur circumference

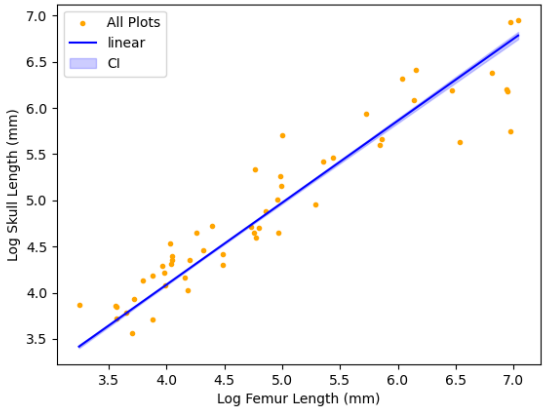

(b) Femur length

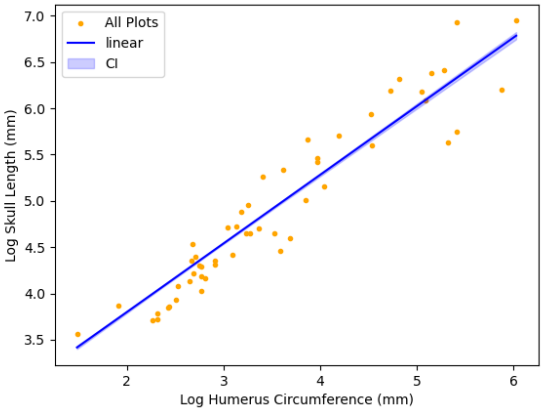

(c) Humerus circumference

Figure 5: Linear regression plots for skull length estimations from femur circumference, femur length, and humerus circumference trained using the Dino Dataset.

mass may be able to support bigger head mass. This hypothesis is consistent with the linear correlation between femur circumference, femur length, and skull length in the Dino Dataset. With disproportions in allometry being hypothesized to be linked to sexual pressure, as seen in preliminary studies, it may be possible that the two clades had similarities in such.

No statistical significance between the distributions fit to Ceratopsian and Quadruped Datasets were detected. With preliminary studies indicating differences in phenotypic variation being affected by localities, the difference in the environments between the mesozoic and cenozoic era may be a cause of such. Analysis of correlation between the anatomical measurements of modern taxa and their diet, such as the plant life, may be helpful in informing the functionalities of head-body size. Such speculation is supported by the relationship between the jaw morphology and head geometry as stated in the preliminary research.

With the uses of principal component analysis for visualization of high dimensional data in preliminary research, it may be of use to visualize measurements of smaller segments of the skull and limbs in future works.

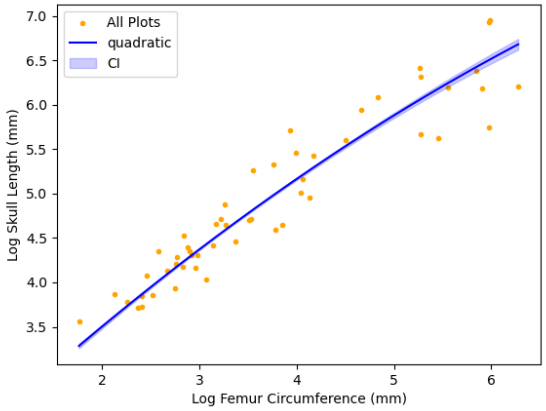

(a) Femur circumference

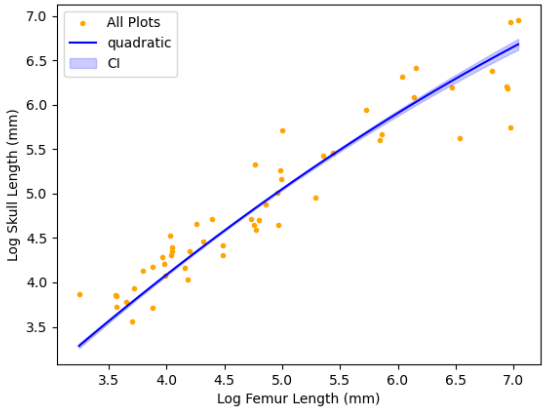

(b) Femur length

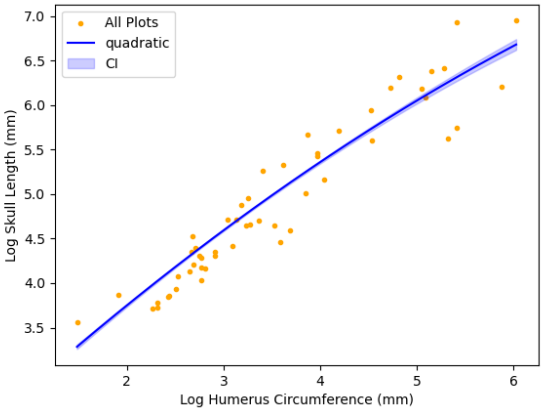

(c) Humerus circumference

Figure 6: Quadratic regression plots for skull length estimations from femur circumference, femur length, and humerus circumference trained using the Dino Dataset.

References

[1] Dean C Adams and Annamaria Nistri. Ontogenetic convergence and evolution of foot morphology in European cave salamanders (Family: Plethodontidae). *BMC Evolutionary Biology*, 10(1):216, 2010.

[2] Russell Bonduriansky. Convergent evolution of sexual shape dimorphism in Diptera. *Journal of Morphology*, 267(5):602–611, 2006.

[3] Russell Bonduriansky and Troy Day. THE EVOLUTION OF STATIC ALLOMETRY IN SEXUALLY SELECTED TRAITS. *Evolution*, 57(11):2450–2458, 2003.

[4] Nicolás E. Campione and David C. Evans. A universal scaling relationship between body mass and proximal limb bone dimensions in quadrupedal terrestrial tetrapods. *BMC Biology*, 10, 2012.

[5] T Alexander Dececchi and Hans C E Larsson. BODY AND LIMB SIZE DISSOCIATION AT THE ORIGIN OF BIRDS: UNCOUPLING ALLOMETRIC CONSTRAINTS ACROSS A MACROEVOLUTIONARY TRANSITION. *Evolution*, 67(9):2741–2752, 2013.

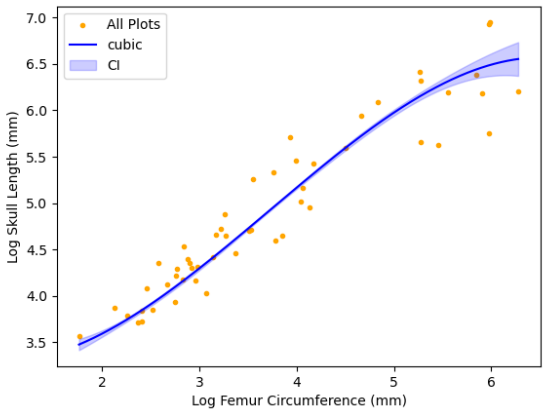

(a) Femur circumference

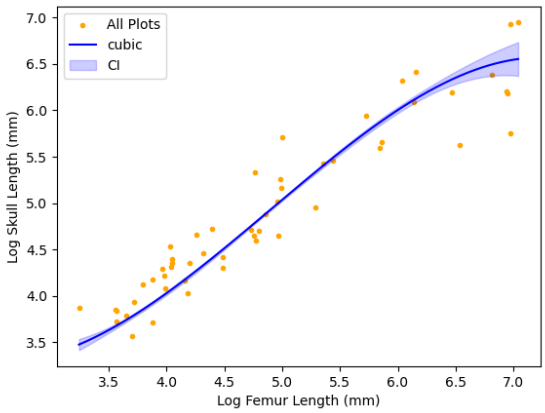

(b) Femur length

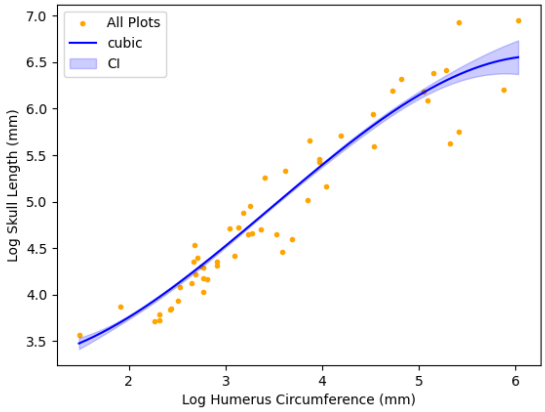

(c) Humerus circumference

Figure 7: Cubic regression plots for skull length estimations from femur circumference, femur length, and humerus circumference trained using the Dino Dataset.

[6] Russell K. Engelman. Author Correction: Occipital condyle width (OCW) is a highly accurate predictor of body mass in therian mammals (BMC Biology, (2022), 20, 1, (37), 10.1186/s12915-021-01224-9). *BMC Biology*, 20(1):1–44, 2022.

[7] Borja Figueirido, Zhijie Jack Tseng, and Alberto Martín-Serra. SKULL SHAPE EVOLUTION IN DUROPHAGOUS CARNIVORANS. *Evolution*, 67(7):1975–1993, 2013.

[8] John R Hutchinson. The evolution of locomotion in archosaurs. *Comptes Rendus Palevol*, 5(3):519–530, 2006.

[9] CHRISTIAN PETER KLINGENBERG. Heterochrony and allometry: the analysis of evolutionary change in ontogeny. *Biological Reviews*, 73(1):79–123, 1998.

[10] Christian Peter Klingenberg and Manfred Zimmermann. Static, Ontogenetic, and Evolutionary Allometry: A Multivariate Comparison in Nine Species of Water Striders. *The American Naturalist*, 140(4):601–620, 1992.

	Validation		Test	
	MSE	CI	MSE	CI
Linear	0.0625	0.0041	0.0847	0.0475
Quadratic	0.0580	0.0039	0.0959	0.0499
Cubic	0.0537	0.0042	0.1455	0.0829

Table 3: Average mean squared error (MSE) losses and their confidence intervals (CI) of linear, quadratic, and cubic regression models for skull length estimations from femur circumference, femur length, and humerus circumference are trained using the Dino Dataset.

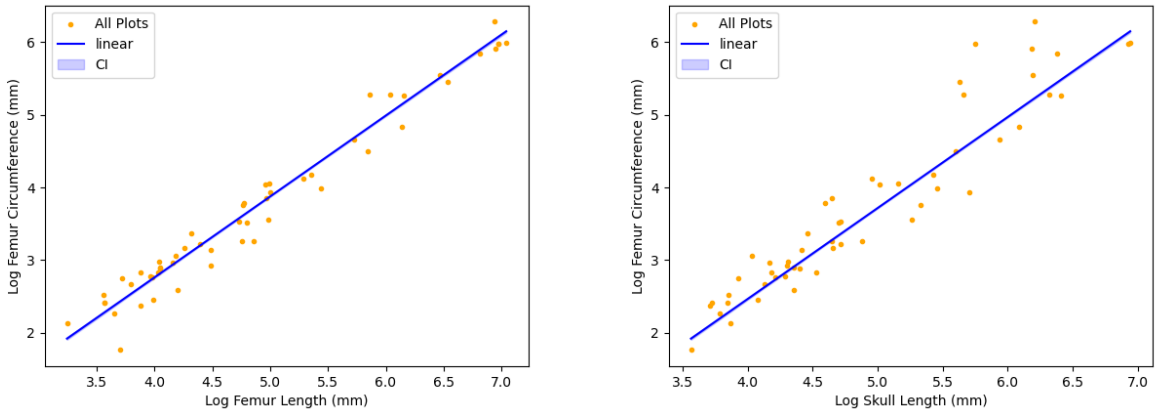

(a) Femur length

(b) Skull length

Figure 8: Linear regression plots for femur circumference estimations from femur length and skull length trained using the Dino Dataset.

[11] Johan Lindgren, Michael W Caldwell, Takuya Konishi, and Luis M Chiappe. Convergent Evolution in Aquatic Tetrapods: Insights from an Exceptional Fossil Mosasaur. *PLOS ONE*, 5(8):1–10, 2010.

[12] Marie Manceau, Vera S Domingues, Catherine R Linnen, Erica Bree Rosenblum, and Hopi E Hoekstra. Convergence in pigmentation at multiple levels: mutations, genes and function. *Philosophical Transactions of the Royal Society B: Biological Sciences*, 365(1552):2439–2450, 2010.

[13] Ariel E Marcy, Elizabeth A Hadly, Emma Sherratt, Kathleen Garland, and Vera Weisbecker. Getting a head in hard soils: Convergent skull evolution and divergent allometric patterns explain shape variation in a highly diverse genus of pocket gophers (Thomomys). *BMC Evolutionary Biology*, 16(1):207, 2016.

[14] Matthew R McCurry, Alistair R Evans, Erich M G Fitzgerald, Justin W Adams, Philip D Clausen, and Colin R McHenry. The remarkable convergence of skull shape in crocodilians and toothed whales. *Proceedings of the Royal Society B: Biological Sciences*, 284(1850):20162348, 2017.

[15] Thomas Minka. Automatic Choice of Dimensionality for PCA. In T Leen, T Dietterich, and V Tresp, editors, *Advances in Neural Information Processing Systems*, volume 13. MIT Press, 2000.

[16] A P Møller, J J Cuervo, J J Soler, and C Zamora-Muoz. Horn asymmetry and fitness in gemsbok, Oryx g. gazella. *Behavioral Ecology*, 7(3):247–253, 1996.

[17] Troy J Myers. Prediction of marsupial body mass. *Australian Journal of Zoology*, 49(2):99–118, 2001.

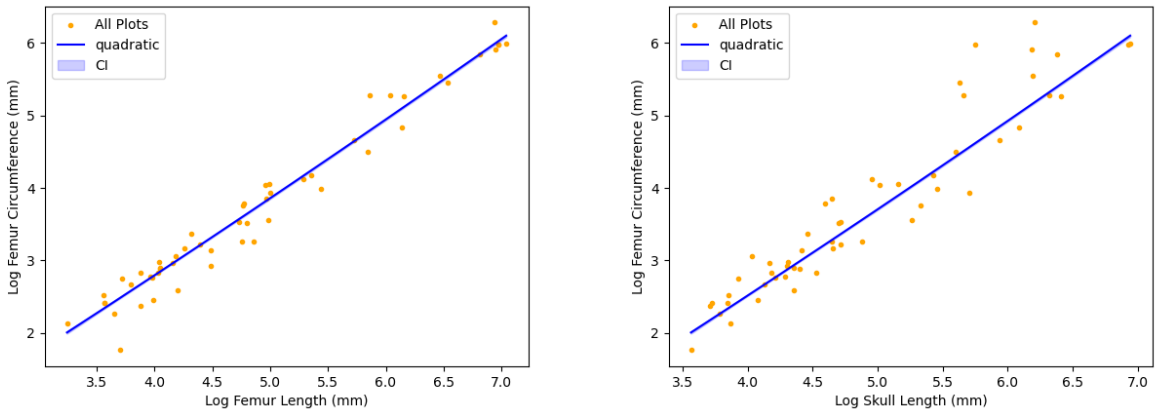

(a) Femur length

(b) Skull length

Figure 9: Quadratic regression plots for femur circumference estimations from femur length and skull length trained using the Dino Dataset.

	KS Test	U-Test
PC 1	0.00	0.00
PC 2	0.00	0.00
PC 3	1.0×10^{-323}	1.3510^{-26}

Table 4: The p-values for the KS and U-test, where the null hypothesis indicates that the parent distribution of the MCMC samples from the models fit to Quadruped and Ceratopsian dataset are equal.

[18] John H Ostrom. Functional Morphology and Evolution of the Ceratopsian Dinosaurs. *Evolution*, 20(3):290–308, 1966.

[19] Paolo Piras, Leonardo Maiorino, Pasquale Raia, Federica Marcolini, Daniele Salvi, Leonardo Vignoli, and Tassos Kotsakis. Functional and phylogenetic constraints in Rhinocerotinae craniodental morphology. *Evolutionary Ecology Research*, 12(8):897–928, 2010.

[20] María C Provensal and Jaime J Polop. Morphometric variation in populations of Calomys musculinus. *Studies on Neotropical Fauna and Environment*, 28(2):95–103, 1993.

[21] Jonathan D Marcot Dale A Russell Reese E. Barrick Michael K. Stoskopf and William J Showers. The thermoregulatory functions of the Triceratops frill and horns: heat flow measured with oxygen isotopes. *Journal of Vertebrate Paleontology*, 18(4):746–750, 1998.

[22] Thomas J Sanger, Liam J Revell, Jeremy J Gibson-Brown, and Jonathan B Losos. Repeated modification of early limb morphogenesis programmes underlies the convergence of relative limb length in ¡i¿Anolis¡/i¿ lizards. *Proceedings of the Royal Society B: Biological Sciences*, 279(1729):739–748, 2012.

[23] Thomas J Sanger, Emma Sherratt, Joel W McGlothlin, I I I Brodie Edmund D., Jonathan B Losos, and Arhat Abzhanov. CONVERGENT EVOLUTION OF SEXUAL DIMORPHISM IN SKULL SHAPE USING DISTINCT DEVELOPMENTAL STRATEGIES. *Evolution*, 67(8):2180–2193, 2013.

[24] David S Strait. Integration, phylogeny, and the hominid cranial base. *American Journal of Physical Anthropology*, 114(4):273–297, 2001.

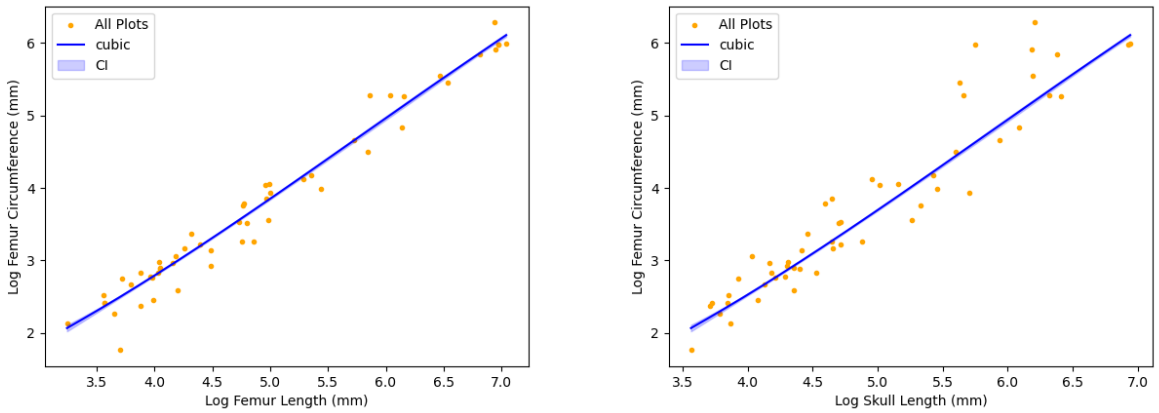

(a) Femur length

(b) Skull length

Figure 10: Cubic regression plots for femur circumference estimations from femur length and skull length trained using the Dino Dataset.

[25] B Van Valkenburgh. Skeletal and dental predictors of body mass in carnivores. *Body size in Mammalian Paleobiology Estimation and biological implications.*, pages 181–205, 1990.

[26] Collin S. Vanburen, Nicolás E. Campione, and David C. Evans. Head size, weaponry, and cervical adaptation: Testing craniocervical evolutionary hypotheses in Ceratopsia. *Evolution*, 69(7):1728–1744, 2015.

[27] Anna I Vickrey, Eric T Domyan, Martin P Horvath, and Michael D Shapiro. Convergent Evolution of Head Crests in Two Domesticated Columbids Is Associated with Different Missense Mutations in EphB2. *Molecular Biology and Evolution*, 32(10):2657–2664, 2015.

[28] Stephen Wroe and Nicholas Milne. CONVERGENCE AND REMARKABLY CONSISTENT CONSTRAINT IN THE EVOLUTION OF CARNIVORE SKULL SHAPE. *Evolution*, 61(5):1251–1260, 2007.

[29] BRUCE A Young, MELISSA Boetig, ANNA Fahey, and ASHLEY Lawrence. The diversity of aquatic locomotion in extant varanoid lizards. In *Proceedings of the second mosasaur meeting, Fort Hays studies, Special issue*, number 3, pages 159–167, 2008.

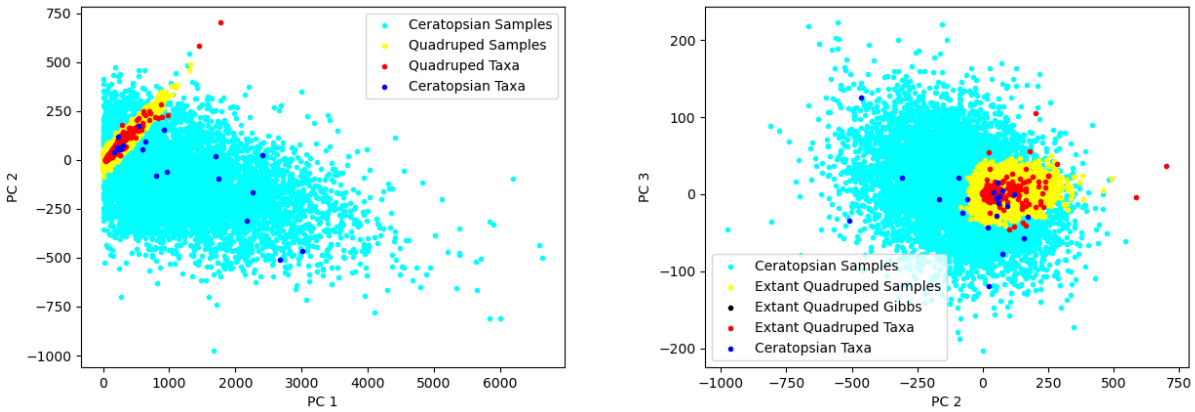

(a) 1st and 2nd principal components

(b) 2nd and 3rd principal components

Figure 11: Plot of all taxa for Ceratopsian and Quadruped Datasets and points sampled from the normal distributions fit to the 2 datasets.

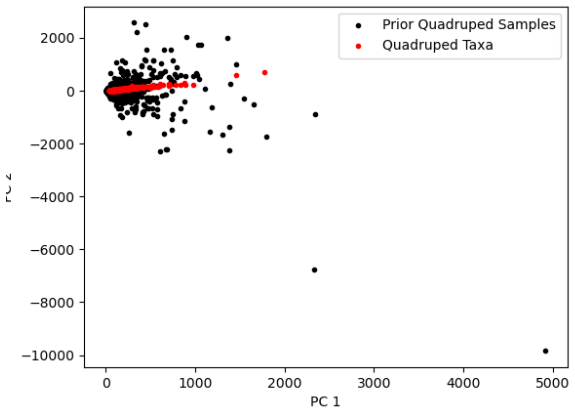

(a) Quadruped 1st and 2nd principal components

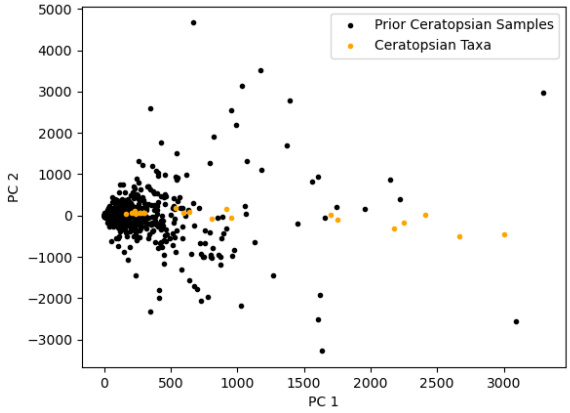

(b) Ceratopsian 1st and 2nd principal components

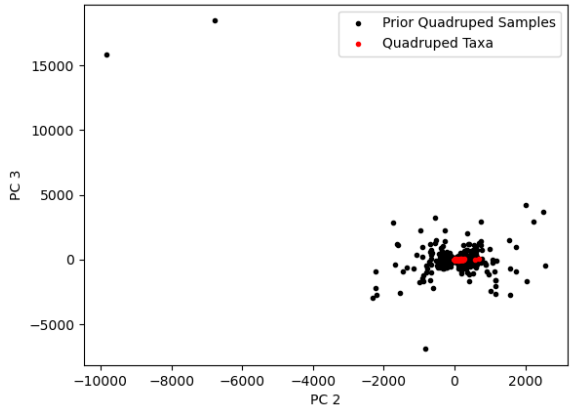

(c) Quadruped 2nd and 3rd principal components

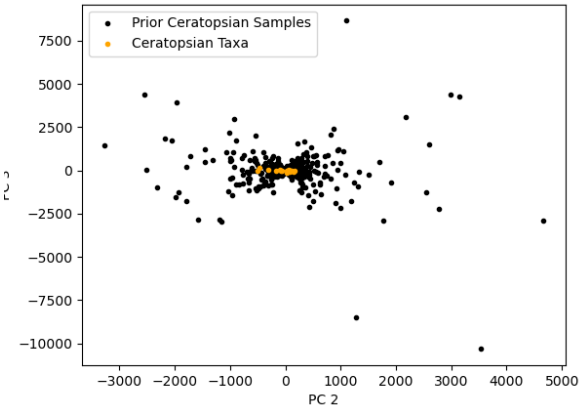

(d) Ceratopsian 2nd and 3rd principal components

Figure 12: Prior predictive check for Quadruped and Ceratopsian Datasets. The original data is indicated in colors, while the sampled priors are indicated in black plots.

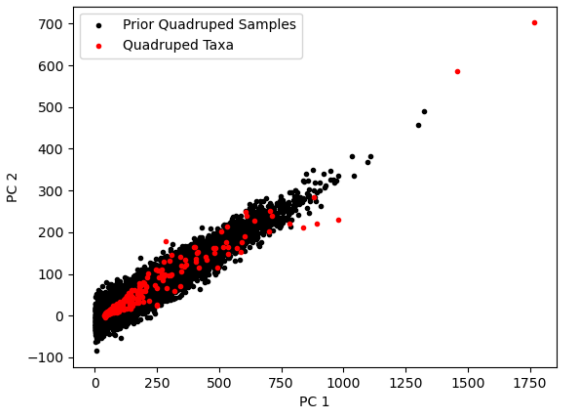

(a) Quadruped 1st and 2nd principal components

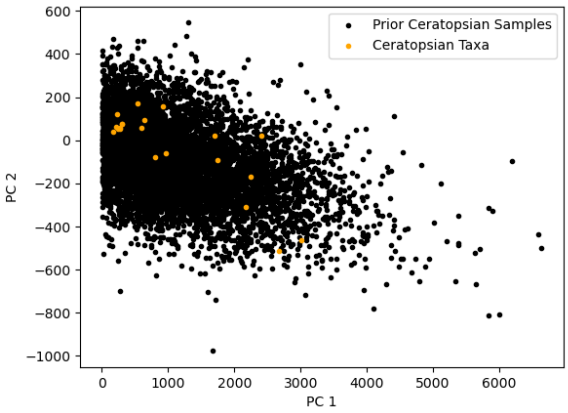

(b) Ceratopsian 1st and 2nd principal components

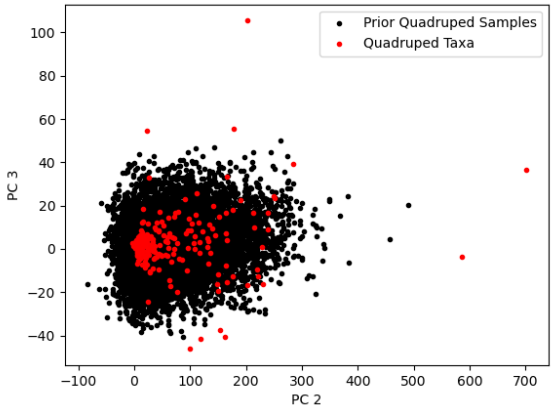

(c) Quadruped 2nd and 3rd principal components

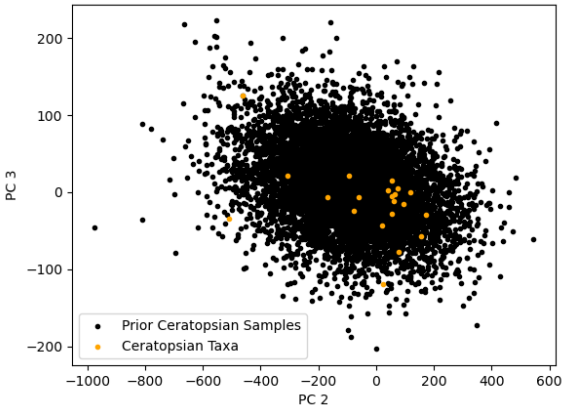

(d) Ceratopsian 2nd and 3rd principal components

Figure 13: Posterior predictive check for Quadruped and Ceratopsian Datasets. The original data is indicated in colors, while the sampled posteriors are indicated in black plots.